IOP PUBLISHING JOURNAL OF PHYSICS G: NUCLEAR AND PARTICLE PHYSICS

J. Phys. G: Nucl. Part. Phys. **34** (2007) 2265–2277 doi:10.1088/0954-3899/34/11/004

Shell effects in damped collisions: a new way to superheavies

Valery Zagrebaev[1] **and Walter Greiner**[2]

[1] Flerov Laboratory of Nuclear Reaction, JINR, Dubna, Moscow Region, Russia
[2] Frankfurt Institute for Advanced Studies, J W Goethe-Universität, Frankfurt, Germany

E-mail: valeri.zagrebaev@jinr.ru

Received 9 August 2007
Published 9 October 2007
Online at stacks.iop.org/JPhysG/34/2265

Abstract

The dynamics of heavy-ion low-energy damped collisions is studied within the model based on the Langevin-type equations. Shell effects on the multi-dimensional potential energy surface play an important role in these reactions. An enhanced yield of nuclides far from the projectile and target masses was found in multi-nucleon transfer reactions due to the shell effects. Our theoretical predictions need experimental confirmation.

1. Introduction

Damped collisions of heavy nuclei were studied extensively about 30 years ago (see, for example, review [1] and references therein). Among others, there had been great interest in the use of heavy-ion transfer reactions with actinide targets to produce new nuclear species in the transactinide region [2–7]. The cross sections were found to decrease very rapidly with the increasing atomic number of surviving target-like fragments—Fm and Md neutron-rich isotopes were produced at the level of 0.1 μb. At that time multi-nucleon transfer reactions were analyzed mainly within the diffusion models [8, 9] in which both fluctuations and shell effects were ignored. At the same time it was also observed that nuclear structure might strongly influence the nucleon flow in the low-energy dissipative collisions of heavy ions. For example, in ^{238}U-induced reactions on ^{110}Pd at about 6 MeV/u bombarding energy an enhanced proton flow along the neutron shells $N_1 = 82$ and $N_2 = 126$ (reached almost simultaneously in target-like and projectile-like fragments) was observed in the distribution of binary reaction products [10]. Note that most experimental studies of damped collisions have been performed at rather high energies (well above the Coulomb barrier) and were not aimed at revealing the shell effects.

Our interest in damped collisions of heavy nuclei is conditioned by the necessity to clarify much better than before the dynamics of heavy nuclear systems at low excitation energies and also by a search for new ways of production of neutron rich superheavy (SH) nuclei and isotopes. SH elements obtained in 'cold' fusion reactions with Pb or Bi target [11] are situated

along the proton drip line, being very neutron-deficient with a short half-life. In the fusion of transactinides with ^{48}Ca more neutron-rich SH nuclei were produced [12] with a much longer half-life. But they are still far from the center of the predicted 'island of stability' formed by the neutron shell around $N = 184$ and proton shells at $Z = 114$ and/or $Z = 120$. In the 'cold' fusion, the cross sections for formation of SH nuclei decrease very fast with the increasing charge of the projectile and become less than 1 pb for $Z \geqslant 112$. On the other hand, the heaviest transactinide, Cf, which can be used as a target in the second method, leads to the SH nucleus with $Z = 118$ being fused with ^{48}Ca. Using the next nearest elements instead of ^{48}Ca (e.g., ^{50}Ti, ^{54}Cr, etc) in fusion reactions with actinides is expected to be less encouraging, although experiments of such a kind are already in progress. In this connection other ways of production of SH elements in the region of the 'island of stability' should be searched for.

In [13, 14] low-energy collisions of very heavy nuclei (^{238}U+^{238}U, ^{232}Th+^{250}Cf, and ^{238}U+^{248}Cm) have been studied and a possibility for the formation of the surviving superheavy long-lived neutron-rich nuclei has been predicted as a matter of principle. It was found that charge and mass transfer strongly depends on the shell structure of the multi-dimensional potential energy surface and also on the values of the fundamental parameters of nuclear dynamics, such as nuclear viscosity and nucleon transfer rate, which are not well determined yet. In spite of the rather good agreement of recent experimental data on ^{238}U+^{238}U collisions [15] with our predictions, more detailed experiments have to be performed in order to study the shell effects in mass transfer in low-energy damped collisions.

The effect of the 'inverse' (antisymmetrizing) quasi-fission process (leading to the formation of SH elements in collisions of transactinides [13]) may also be studied in experiments with less heavy nuclei. In this paper we analyze in detail one of such reactions, namely ^{160}Gd+^{186}W. The choice of the projectile and target nuclei is conditioned by the fact that these nuclei are located just between the closed shells ($Z_1 = 50, N_1 = 82$) and ($Z_2 = 82, N_2 = 126$) which, as we expected, should play a significant role in the nucleon transfer process. Comparison of our predictions with experimental probability for multi-nucleon transfer (which can be measured for this reaction much easier as compared to U+Cm collisions, for example) may significantly help us to perform a realistic estimation of a possibility for the synthesis of long-living neutron-rich SH nuclei in low-energy damped collisions of heavy ions (also induced by the accelerated neutron-rich fission fragments).

2. The model

We performed a calculation based on the dynamical model proposed in [14, 16]. The distance between the nuclear centers R (corresponding to the elongation of a mono-nucleus), the dynamic spheroidal-type surface deformations β_1 and β_2, the mutual in-plane orientations of deformed nuclei φ_1 and φ_2, and the mass asymmetry $\eta = \frac{A_1 - A_2}{A_1 + A_2}$ are the relevant degrees of freedom for the description of deep inelastic (DI) scattering and fusion–fission dynamics. The interaction potential of separated nuclei is calculated rather easily within the folding procedure with effective nucleon–nucleon interaction or parameterized, e.g., by the proximity potential [17]. Of course, some uncertainty remains here, but the height of the Coulomb barrier obtained in these models coincides with the empirical Bass parametrization [18] within 1 or 2 MeV. The dynamic deformations of colliding spherical nuclei and the mutual orientation of statically deformed nuclei significantly affect their interaction changing the height of the Coulomb barrier by more than 10 MeV. It is caused mainly by a strong dependence of the distance between nuclear surfaces on the deformations and orientations of nuclei. Geometrical effects due to a change in the curvature of deformed nuclear surfaces are also important here and should be taken into account if the phenomenological nucleus–nucleus potential is used.

After contact the mechanism of interaction between two colliding nuclei becomes more complicated. For fast collisions ($E/A \sim \varepsilon_{\rm Fermi}$ or higher) the nucleus–nucleus potential, $V_{\rm diab}$, should reveal a strong repulsion at short distances protecting the 'frozen' nuclei to penetrate each other and form a nuclear matter with double density (diabatic conditions, sudden potential [19]). For slow collisions (near-barrier energies), when nucleons have enough time to reach equilibrium distribution (adiabatic conditions), the nucleus–nucleus potential energy, $V_{\rm adiab}$, is quite different. Thus, for the nucleus–nucleus collisions at energies above the Coulomb barrier we need to use a time-dependent potential energy, which, after contact, gradually transforms from a diabatic potential energy into an adiabatic one: $V = V_{\rm diab}[1 - f(t)] + V_{\rm adiab} f(t)$ [16]. Here t is the time of interaction and $f(t)$ is a smoothing function satisfying the conditions $f(t = 0) = 0$ and $f(t \gg \tau_{\rm relax}) = 1$.

We found that the shape of this function does not influence the results of calculations. Only the relaxation time $\tau_{\rm relax}$ is of practical importance. Its value was estimated earlier at the level of 10^{-21} s [20]. Recently even a shorter value of 0.5×10^{-21} s has been found for this parameter [21]. So the fast relaxation of a diabatic potential into an adiabatic one means that at slow near-barrier collisions just the adiabatic potential mainly regulates the whole reaction process. Here we used the empirical smoothing function $f(t) = \frac{1}{2}\left[1 - \cos\left(\pi \frac{t}{\tau_{\rm relax}}\right)\right]$ with $\tau_{\rm relax} = 2 \times 10^{-21}$ s. We assume that the difference between diabatic and adiabatic potential energy transforms into an excitation of the nuclear system. Note that at $t > \tau_{\rm relax}$ due to a strong nuclear viscosity almost all kinetic energy is dissipated and an overdamped regime of motion takes place (see below).

For the diabatic potential energy we used the proximity potential [17] (with the geometrical factor depending on nuclear deformations) and the semi-empirical two-core model of nucleon collectivization [22, 23] based on the two-center shell model idea [24] was used for the calculation of the adiabatic potential energy. Experimental binding energies of two cores are used here for the intermediate shapes, thus giving us the 'true' values of the shell corrections. The value of the shell corrections depends also on the dynamic deformation of two fragments (see details in [14]). This adiabatic potential is used as a bottom value of the potential energy surface of the nuclear system in a space of collective degrees of freedom. The difference between the total energy and a sum of this potential energy surface and kinetic energy is treated as an excitation energy of the nuclear system (its temperature). This excitation (gradually appearing due to friction forces when nuclei approach each other) leads to fluctuations of the collective degrees of freedom, which may be taken into account by the random forces within the Langevin-type equations of motion.

It is important to note that we use the same degrees of freedom, the same potential energy surface and the same set of equations of motion for the description of all the reaction stages. In contrast with other models, we need not split artificially the whole reaction process into several stages when we consider strongly coupled DI, QF and CN formation processes. Initial conditions are formulated quite unambiguously at a large distance (at a given impact parameter, randomly chosen orientations of the nuclei and parameters of zero-vibrations in their ground states) where only the Coulomb interaction determines the motion. Then the evolution of the nuclear system is traced in the multi-dimensional space of collective variables up to the formation of CN or re-separation into the new fragments in DI or QF channels.

For all the degrees of freedom, with the exception of the mass asymmetry η, we used the usual Langevin equations of motion and for overlapping nuclei the inertia parameters, μ_R and μ_β, were calculated within the Werner–Wheeler approach [25]. The same nuclear shapes were used for the calculation of the potential energy and inertia parameters (see details in [23]). Note that for the studied reactions (low-energy collisions of very heavy nuclei) the overlapping of the fragments is rather small (the absence of the noticeable potential pocket) and, thus, the

inertia parameters are very close to the two-body limits. To simplify the calculations, and interested mostly in the peripheral collisions, we here ignored the off-diagonal terms of the inertia tensor.

At the moment we cannot numerically solve a problem with two independent dynamic deformations of the fragments (four-dimensional potential energy surface). To reduce the number of the variables we restricted ourselves to the consideration of only one spheroidal dynamic deformation β instead of two independent deformations β_1 and β_2. We assumed 'equality of forces', i.e., $C_1\beta_1 = C_2\beta_2$, where $C_{1,2}$ are the LDM stiffness parameters of the fragments. Using this ratio and $\beta_1 + \beta_2 = 2\beta$ the deformations of the fragments can be derived from the common variable β. Removing this simplification could be rather important.

Mass asymmetry is a discrete variable by its nature. Thus nucleon transfer may hardly be described by a Newtonian-type equation. Moreover, the corresponding inertia parameter μ_η, being calculated within the Werner–Wheeler approach, becomes infinite at the contact (scission) point and for separated nuclei (see also a discussion of this problem within the fragmentation model [26]). The master equation for the distribution function seems to be quite good for the description of nucleon transfer [27, 28]. However, this equation defines the time evolution of the distribution function (not of the variable η itself!), and it cannot be used directly in a common set of coupled differential equations for the coordinates R and β.

In [16] the Langevin-type equation for the mass asymmetry

$$\frac{\mathrm{d}\eta}{\mathrm{d}t} = \frac{2}{A_{CN}} D_A^{(1)}(\eta) + \frac{2}{A_{CN}} \sqrt{D_A^{(2)}(\eta)}\,\Gamma(t) \tag{1}$$

has been derived from the corresponding master equation for the distribution function. Here $\Gamma(t)$ is the normalized random variable with Gaussian distribution, $\langle \Gamma(t) \rangle = 0$, $\langle \Gamma(t)\,\Gamma(t') \rangle = 2\delta(t - t')$, and $D_A^{(1)}$, $D_A^{(2)}$ are the transport coefficients. A is the number of nucleons in one of the fragments and $\eta = (2A - A_{CN})/A_{CN}$.

Assuming that sequential nucleon transfers play a main role in mass rearrangement, i.e. $A' = A \pm 1$, we have

$$\begin{aligned} D_A^{(1)} &= \lambda(A \to A+1) - \lambda(A \to A-1), \\ D_A^{(2)} &= \tfrac{1}{2}[\lambda(A \to A+1) + \lambda(A \to A-1)]. \end{aligned} \tag{2}$$

For nuclei in contact the macroscopic transition probability $\lambda(A \to A' = A \pm 1)$ is defined by nuclear level density, $\lambda^{(\pm)} = \lambda_0 \sqrt{\rho(A \pm 1)/\rho(A)}$. The shell correction in the level density parameter is damped in a usual way with increasing the excitation energy.

λ_0 is the nucleon transfer rate ($\sim 10^{22}$ s^{-1} [27, 28]), which may, in principle, depend on the excitation energy (the same holds for the diffuseness coefficient $D_A^{(2)}$). This feature, however, is not completely clear. In [27] the mass diffusion coefficient was assumed to be independent of excitation energy, whereas microscopic consideration yields its square root dependence on nuclear temperature [29]. A linear dependence of the mass diffusion coefficient on the temperature was also used [30]. Here we treat the nucleon transfer rate λ_0 as a parameter of the model chosen from the analysis of available experimental data on DI scattering.

Nucleon transfer for slightly separated nuclei is also rather probable. This intermediate nucleon exchange plays an important role in sub-barrier fusion processes [31, 32] and has to be taken into account in equation (1). It can be treated by using the following final expression for the transition probability:

$$\lambda^{(\pm)} = \lambda_0 \sqrt{\frac{\rho(A \pm 1)}{\rho(A)}}\, P_{\mathrm{tr}}(R, \beta, A \to A \pm 1). \tag{3}$$

Here $P_{\mathrm{tr}}(R, \beta, A \to A \pm 1)$ is the probability of one-nucleon transfer, which depends on the distance between the nuclear surfaces. This probability goes exponentially to zero at $R \to \infty$

and it is equal to unity for overlapping nuclei. In our calculations we used the semiclassical approximation for $P_{\rm tr}$ proposed in [31]. Equation (1) along with (3) defines the continuous change of mass asymmetry in the whole space (obviously, $\frac{{\rm d}\eta}{{\rm d}t} \to 0$ for far separated nuclei).

The uncertainty in the strength of nuclear viscosity (nuclear friction) and in its form-factor is also very large. Moreover, microscopic analysis shows that nuclear viscosity may strongly depend on nuclear temperature [33]. Analyzing experimental data on DI scattering of heavy ions we prefer to treat nuclear friction on a phenomenological base using appropriate strength parameters [14, 16]. However, there are almost no experimental data on low-energy (near to the Coulomb barrier) damped collisions with low excitations (low temperatures) of the fragments which significantly complicates the choice of the nuclear viscosity parameters.

The double differential cross-sections of all the processes are calculated as follows:

$$\frac{{\rm d}^2\sigma_\eta}{{\rm d}\Omega\,{\rm d}E}(E,\theta) = \int_0^\infty b\,{\rm d}b \frac{\Delta N_\eta(b,E,\theta)}{N_{\rm tot}(b)} \frac{1}{\sin(\theta)\Delta\theta\Delta E}. \tag{4}$$

Here $\Delta N_\eta(b, E, \theta)$ is the number of events at a given impact parameter b in which the system enters into the channel η (definite mass asymmetry value) with kinetic energy in the region $(E, E + \Delta E)$ and center-of-mass outgoing angle in the region $(\theta, \theta + \Delta\theta)$; $N_{\rm tot}(b)$ is the total number of simulated events for a given value of the impact parameter. Expression (4) describes the mass, energy and angular distributions of the *primary* fragments formed in the binary reaction. Subsequent de-excitation cascades of these fragments via fission and emission of light particles and gamma-rays were taken into account explicitly for each event within the statistical model leading to the *final* mass and energy distributions of the reaction products. The sharing of the excitation energy between the primary fragments was assumed to be proportional to their masses. For both excited fragments the multi-step decay cascade was analyzed taking into account the competition between the evaporation of neutrons and/or protons and fission. At the final stage of the evaporation cascade $\left(E^* < E_n^{\rm sep}\right)$ the competition between γ-emission and fission was taken into account. All the corresponding widths of decay were calculated in accordance with [34].

3. Shell effects in mass transfer

In figure 1 the multi-dimensional adiabatic driving potential is shown in the spaces of 'elongation–mass asymmetry' and 'elongation–deformation' for the axially symmetric nuclear system formed in the collision of ^{160}Gd+^{186}W. There is no potential pocket for this heavy nuclear system. However, as can be seen from figure 1, the potential energy at the contact point is rather flat (particularly along the deformation coordinate), which means that the nuclei may keep in touch a long time due to fluctuations and nucleon transfer.

We used the same value of $\mu_0 = 1 \times 10^{-22}$ MeV s fm^{-3} for the nuclear viscosity strength which was found appropriate for the description of the experimental energy, mass and angular distributions measured for low-energy DI scattering of ^{136}Xe from ^{209}Bi [14]. The values of the parameters for the nuclear friction form-factor have been taken from [16]. The nucleon transfer rate was fixed at $\lambda_0 = 0.06 \times 10^{22}$ s^{-1}, a little bit less than for the description of Xe+Bi experimental data [14] to avoid an overestimation of the shell effects in mass transfer.

One of the 'trajectories' corresponding to the evolution of the nuclear system formed in the collision of ^{160}Gd with ^{186}W at zero impact parameter and 460 MeV center-of mass energy (corresponding to the Bass barrier [18]) is shown in figure 2. Moving along this trajectory the nuclear system was in contact during the 0.5×10^{-20} s, the time from the moment when colliding nuclei (Gd+W, $\eta = 0.075$) came in touch in the entrance channel and up to the moment of scission (at $\eta = 0.013$) in the exit one.

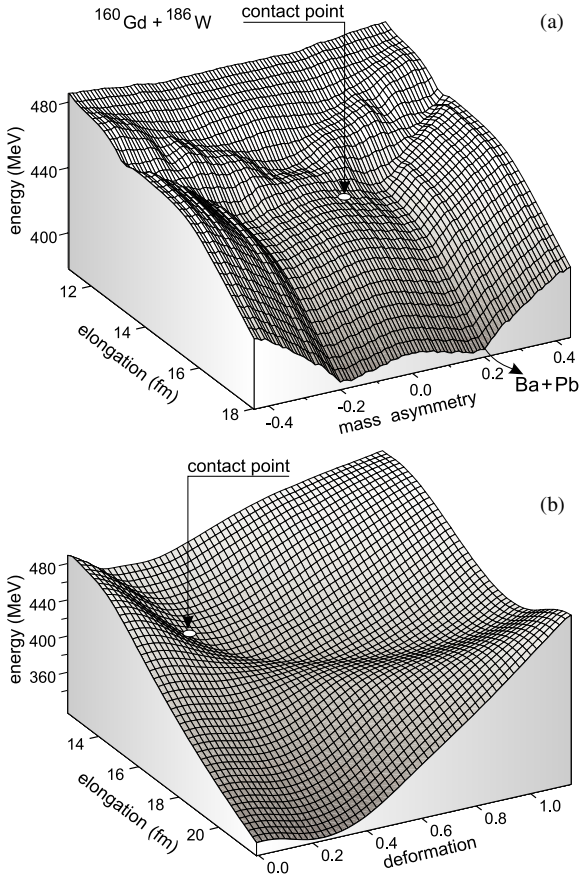

Figure 1. Potential energy surface of the nuclear system formed in the collision of ^{160}Gd+^{186}W. (a) Dependence on elongation and mass asymmetry (deformation is fixed at $\beta = 0.2$); (b) dependence on elongation and deformation at a fixed value of the mass asymmetry, $\eta = 0.075$ (entrance channel).

The interaction time is one of the most important characteristics of nuclear reactions, although it cannot be measured directly. The reaction time distribution in damped collisions of ^{160}Gd with ^{186}W calculated at 460 MeV center-of-mass beam energy is shown in figure 3. An interaction time of several units of 10^{-21} s is quite enough for the kinetic energy to be totally dissipated and a large amount of mass can be rearranged during this time. Due to a strong nuclear viscosity, after contact the system creeps along the bottom of the driving potential and the shell effects have to play a significant role in the process of mass transfer.

In figure 4 the potential energy is shown at a contact configuration depending on mass asymmetry (mass transfer). As can be seen from figure 1(b) the potential energy strongly depends on the deformations of touching fragments. However, even for rather large deformations the shell effects are still quite visible. This was already recognized within an early version of the two-center shell model [24]. In particular, the configuration of ^{138}Ba+^{208}Pb has much lower potential energy compared with the nearest ones due to the influence of the neutron ($N = 82$ and $N = 126$) and proton ($Z = 82$) shells.

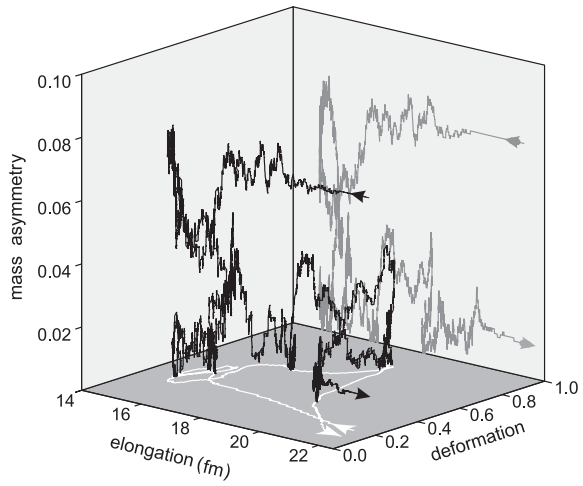

Figure 2. Typical trajectory shown evolution of the nuclear system formed in the collision of ^{160}Gd+^{186}W at 460 MeV center-of mass energy (zero impact parameter) in the space of 'elongation–deformation–mass asymmetry'.

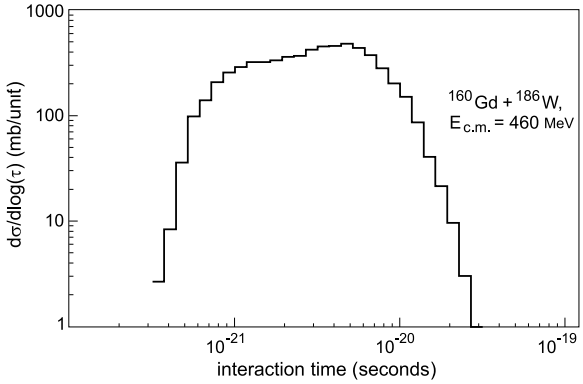

Figure 3. Reaction time distribution for the ^{160}Gd+^{186}W collisions at 460 MeV center-of mass energy.

The mass distributions of the primary fragments in the ^{160}Gd+^{186}W reaction calculated with and without the shell corrections to the potential energy are shown in figure 5. Only the events with energy loss higher than 15 MeV were taken into account to exclude the contribution from the quasi-elastic scattering. As can be seen at near barrier collision energies, the shell effects really play a very important role and may increase by two orders of magnitude the yield of reaction products even for a transfer of 20 nucleons.

For more asymmetric combinations (such as Ca+Cm and so on) the shell effects, caused by the magic nuclei located between the colliding partners (^{132}Sn and ^{208}Pb in the case of Ca+Cm collision), reveal themselves as the quasi-fission process—an unusual mass distribution of the fission-like fragments of compound nucleus (CN) with an increased yield of nuclei with closed shells (see, for example, [35]). The process we discuss here is rather similar. However, there are two important distinctions. First, CN is not formed at all in a collision of very

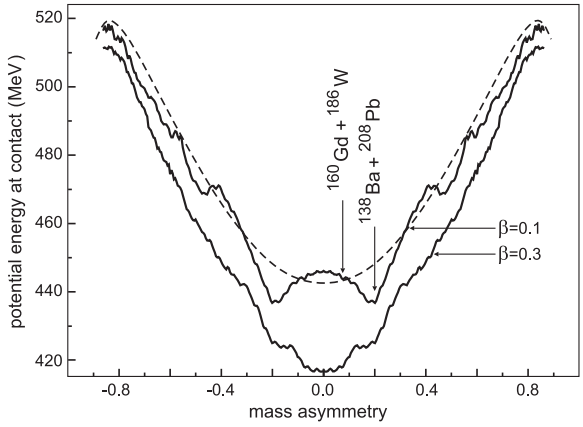

Figure 4. Potential energy at contact configuration of different fragments formed from ^{160}Gd and ^{186}W. The deformation is fixed at $\beta = 0.1$ (upper curves) and $\beta = 0.3$ (lower curve). The dashed curve shows the potential energy without shell corrections at $\beta = 0.1$.

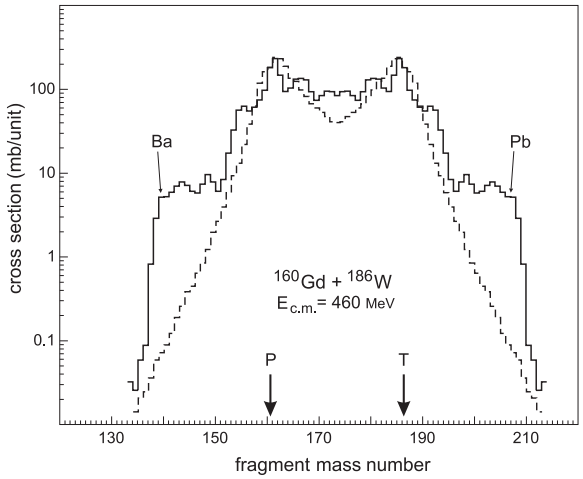

Figure 5. Primary fragment mass distribution in the ^{160}Gd+^{186}W reaction at 460 MeV center-of mass energy calculated with (solid) and without (dashed histogram) shell corrections in potential energy.

heavy nuclei. This is not a fusion–fission process, as in the case of Ca+Cm collision, but a DI (damped) reaction. Second, the magic nuclei ($Z = 50$, $N = 82$) and ($Z = 82$, $N = 126$) are located here from the outside of the colliding partners. Thus the shell effects drive to increase the initial mass asymmetry—that is why we name this process 'inverse (antisymmetrizing) quasi-fission'.

This process is very interesting and it has not yet been studied experimentally. A choice of the initial nuclear combination is very important here. Colliding partners should be rather far from the closed shell nuclei and the initial energy should be rather low to prevent the shell effects of smearing. If the shell effects for the mass transfer in low-energy damped collisions of heavy ions will be found as high as we predict, then such reactions can be used also for the production of SH nuclei [13, 14]. In collisions of transactinides (such as U+Cm, for example)

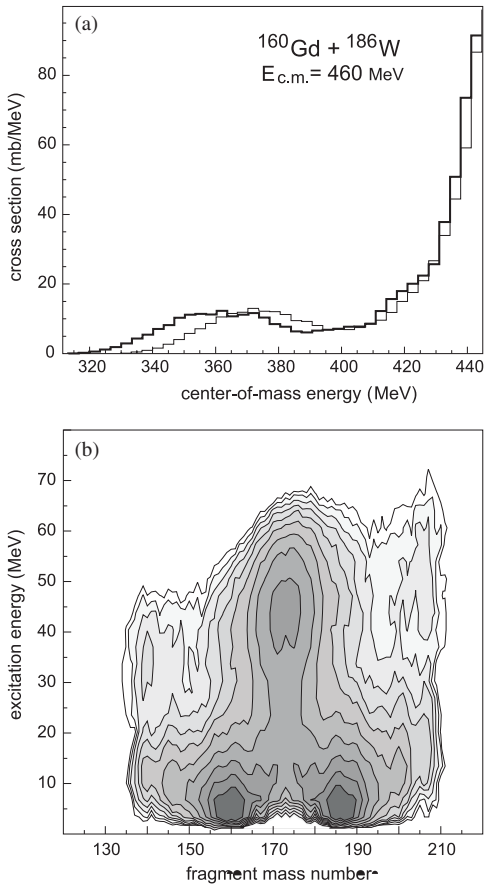

Figure 6. (a) Total kinetic energy distribution of primary (thin) and final (thick histogram) products of the ^{160}Gd+^{186}W reaction at 460 MeV center-of mass energy. (b) Excitation energy of primary fragments.

one of the fragments (donor) may decrease its mass slipping into the lead valley whereas the other (acceptor) will increase its mass transforming into a SH nucleus. It is important that a SH nucleus obtained in such a way will be more neutron rich than those obtained in complete fusion reactions (just due to conservation of proton and neutron numbers). Reactions with transactinides are rather difficult to be performed (though quite possible), whereas low-energy damped collisions of intermediate mass nuclei (such as Gd+W and others) are less difficult for experimental study. One may expect that the antisymmetrizing shell effect will be similar in both cases.

The choice of a low beam energy (close to the Coulomb barrier) is important not only to keep the shell corrections of smearing out but also to obtain heavy reaction fragments with low excitation energy giving them a chance to survive in the de-excitation process with evaporation of light particles in competition with fission. The total kinetic energy distribution and the excitation energies of the primary fragments formed in the ^{160}Gd+^{186}W reaction at 460 MeV center-of mass energy are shown in figure 6 (we assumed excitation energy sharing proportional to the masses of reaction products). As can be seen, the excitation energy of heavy fragments produced in this reaction is not higher than a few tens of MeV. Also there

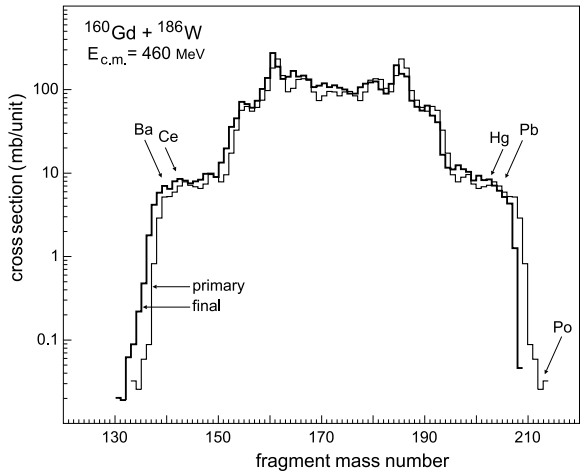

Figure 7. Final (thick) and primary (thin histogram) fragment mass distributions in the ^{160}Gd+^{186}W reaction at 460 MeV center-of mass energy.

are many events in which the heaviest fragments have low excitation energy in spite of about 20 transferred nucleons. For the considered reaction the heaviest fragments are located in the lead region and have rather high fission barriers preventing them from fission. In collisions of transactinide nuclei most of the produced SH elements will definitely undergo fission. However, at excitation energies of a few tens of MeV there is still some chance for these nuclei to survive due to the cooling process with evaporation of neutrons [13, 14].

Knowing the excitation energies and angular momenta of the primary fragments formed in the reaction, we then used the statistical model for the analysis of the multi-step evaporation cascade competing with fission. Only the evaporation of neutrons and protons was taken into account and all the corresponding decay widths were calculated in accordance with [34]. The analysis of this evaporation cascade needs the longest computation time and we tested only 10^6 events, which allowed us to obtain an appropriate estimation of the cross sections for the formation of primary fragments up to the level of 0.1 mb.

The final fragment mass distribution for the ^{160}Gd+^{186}W reaction is shown in figure 7. Rather low excitation energies (result of low bombarding energy) do not very much distort the primary fragment mass distribution (except for the yield of very heavy nuclei). Pronounced shoulders of the mass distribution in the regions of $A_1 = 140$ and $A_2 = 200$ clearly testify for the strong influence of the shell effects in low-energy damped collisions of heavy ions.

Increasing the beam energy leads, in general, to an increase of the mass transfer cross sections. At the same time the excitation energy of the primary fragments formed in binary reaction channels also increases. This leads to a widening of the isotope distribution for a given element and to a shift of this distribution to lighter masses due to a larger number of evaporated neutrons. The calculated distributions of the lead isotopes produced in the ^{160}Gd+^{186}W reaction at two different beam energies are shown in figure 8.

In contrast to collisions of transactinide nuclei, an experimental study of the low-energy ^{160}Gd+^{186}W reaction is not difficult to perform. The angular–mass distribution of the final reaction fragments in the laboratory system is shown in figure 9. As can be seen, the laboratory angles in the region of 80°–100° may be chosen to detect the left (light) shoulder of the mass distribution and to avoid detecting the products of quasi-elastic scattering. Note

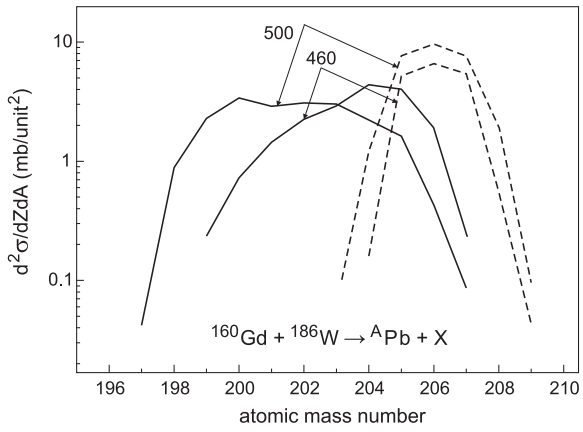

Figure 8. Yield of the lead isotopes in the ^{160}Gd+^{186}W reaction at 460 and 500 MeV center-of mass incident energies. The dashed and solid curves show the yields of primary and final nuclei (after neutron evaporation cascade), respectively.

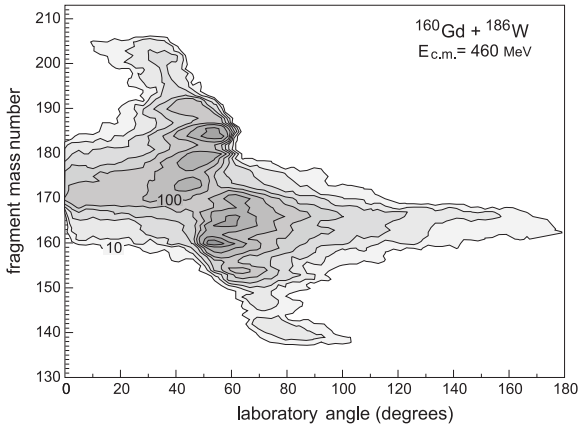

Figure 9. Laboratory-system angular-mass distribution of the final fragments formed in the ^{160}Gd+^{186}W damped collisions. The landscape is drawn in logarithmic scale (see relative units near the two contours). Only events with energy loss larger than 15 MeV are shown.

that other combinations of colliding nuclei (e.g., ^{154}Sm+^{192}Os with $\Delta A = 16$ to reach ^{208}Pb, or ^{170}Er+^{176}Yb with $\Delta A = 32$) could also be interesting for experimental study.

4. Conclusion

We found that shell effects are playing a very important role in low-energy damped collisions of heavy ions. At the beam energies close to the Coulomb barrier (to give a chance for colliding nuclei to come into contact) in reactions with nuclei far from the closed shells the fragment mass distribution should strongly deviate from a monotonous decrease with increasing mass transfer. The yield of the reaction products in the regions of magic nuclei may be enhanced by two orders of magnitude. Experimental observation of this effect is quite important! First,

it would give us a better understanding of the low-energy dynamics of heavy nuclear systems and clarify to what extend the shell effects influence the mass transfer in damped collisions of heavy ions. Second, the experimentally measured enhancement factor in the yield of closed shell nuclei might allow us to make more accurate predictions (and simple extrapolations) of this effect for other nuclear combinations (which are more difficult for experimental study). If experimental observations confirm our predictions, then the production of long-living neutron-rich SH nuclei in collisions of transuranium ions will be really possible due to a large mass and charge rearrangement in the inverse (anti-symmetrizing) quasi-fission process caused by the $Z = 82$ and $N = 126$ nuclear shells.

Acknowledgments

We are grateful to Professors M Itkis and Yu Oganessian for a constructive discussion of the problem. The work was supported partially by the DFG-RFBR collaboration project under grant no 04-02-04008.

References

[1] Schröder W U and Huizenga J R Damped nuclear reactions *Treatise on Heavy-Ion Science* vol 2 ed D A Bromley (New York: Plenum) p 140
[2] Hulet E K *et al* 1977 *Phys. Rev. Lett.* **39** 385
[3] Schädel M *et al* 1978 *Phys. Rev. Lett.* **41** 469
[4] Freiesleben H, Hildenbrand K D, Pühlhofer F, Schneider W F W, Bock R, Harrach D V and Specht H J 1979 *Z. Phys.* A **292** 171
[5] Schädel M *et al* 1982 *Phys. Rev. Lett.* **48** 852
[6] Moody K J, Lee D, Welch R B, Gregorich K E, Seaborg G T, Lougheed R W and Hulet E K 1986 *Phys. Rev.* C **33** 1315
[7] Welch R B, Moody K J, Gregorich K E, Lee D, Seaborg G T, Lougheed R W and Hulet E K 1987 *Phys. Rev.* C **35** 204
[8] Wolschin G and Nörenberg W 1978 *Z. Phys.* A **284** 209
[9] Riedel C and Nörenberg W 1979 *Z. Phys.* A **290** 385
[10] Mayer W, Beier G, Friese J, Henning W, Kienle P, Körner H J, Mayer W A, Müller L, Rosner G and Wagner W 1985 *Phys. Lett.* B **152** 162
[11] Hofmann S and Münzenberg G 2000 *Rev. Mod. Phys.* **72** 733
[12] Oganessian Yu Ts *et al* 2004 *Phys. Rev.* C **70** 064609
[13] Zagrebaev V I, Oganessian Yu Ts, Itkis M G and Greiner W 2006 *Phys. Rev.* C **73** 031602(R)
[14] Zagrebaev V and Greiner W 2007 *J. Phys. G: Nucl. Part. Phys.* **34** 1
[15] Villari A C C *et al* 2006 *Proc. Tours Symp. on Nuclear Physics VI (France, 2006), AIP Conf. Proc.* **891** 60
[16] Zagrebaev V and Greiner W 2005 *J. Phys. G: Nucl. Part. Phys.* **31** 825
[17] Blocki J, Randrup J, Swiatecki W J and Tsang C F 1977 *Ann. Phys., NY* **105** 427
[18] Bass R 1980 *Nuclear Reactions with Heavy Ions* (Berlin: Springer) p 326
[19] Scheid W, Ligensa R and Greiner W 1968 *Phys. Rev. Lett.* **21** 1479
[20] Bertsch G F 1978 *Z. Phys.* A **289** 103
Cassing W and Nörenberg W 1983 *Nucl. Phys.* A **401** 467
[21] Diaz-Torres A 2006 *Phys. Rev.* C **74** 064601
[22] Zagrebaev V I 2001 *Phys. Rev.* C **64** 034606
[23] Zagrebaev V I 2004 *Proc. Tours Symp. on Nuclear Physics (France, 2003), AIP Conf. Proc.* **704** 31
[24] Mosel U, Maruhn J and Greiner W 1971 *Phys. Lett.* B **34** 587
Maruhn J and Greiner W 1972 *Z. Phys.* **251** 431
[25] Werner F G and Wheeler J A unpublished
Davies K T R, Sierk A J and Nix J R 1976 *Phys. Rev.* C **13** 2385
[26] Fink H J, Maruhn J, Scheid W and Greiner W 1974 *Z. Phys.* **268** 321
[27] Nörenberg W 1974 *Phys. Lett.* B **52** 289
[28] Moretto L G and Sventek J S 1975 *Phys. Lett.* B **58** 26
[29] Ayik S, Schürmann B and Nörenberg W 1976 *Z. Phys.* A **279** 174

[30] Schmidt R and Wolschin G 1980 *Z. Phys.* A **296** 215
[31] Zagrebaev V I 2003 *Phys. Rev.* C **67** 061601(R)
[32] Zagrebaev V I, Samarin V V and Greiner W 2007 *Phys. Rev.* C **75** 035809
[33] Hofmann H 1997 *Phys. Rep.* **284** 137
Ivanyuk F A 2000 *Proc. on Dynamical Aspects of Nuclear Fission (Slovakia, 1998)* ed Yu Ts Oganessian, J Kliman and Š Gmuca (Singapore: World Scientific) p 424
[34] Zagrebaev V I, Aritomo Y, Itkis M G, Oganessian Yu Ts and Ohta M 2002 *Phys. Rev.* C **65** 014607
[35] Itkis M G *et al* 2004 *Nucl. Phys.* A **734** 136